

On the Origin of HD149026b

M. Ikoma

*Research Center for the Evolving Earth and Planets, Tokyo Institute of Technology, Ookayama,
Meguro-ku, Tokyo 152-8551, Japan*

mikoma@geo.titech.ac.jp

T. Guillot

Observatoire de la Côte d'Azur, CNRS UMR 6202, BP 4229, 06304 Nice Cedex 4, France

H. Genda, T. Tanigawa, & S. Ida

*Earth and Planetary Sciences, Tokyo Institute of Technology, Ookayama, Meguro-ku, Tokyo
152-8551, Japan*

ABSTRACT

The high density of the recently discovered close-in extrasolar planet HD149026b suggests the presence of a huge core in the planet, which challenges planet formation theory. We first derive constraints on the amount of heavy elements and hydrogen/helium present in the planet: We find that preferred values of the core mass are between 50 and $80M_{\oplus}$, although a minimum value of the core mass is $\sim 35M_{\oplus}$ in the extreme case of formation of the planet at > 0.5 AU, followed by late inward migration after > 1 Ga and negligible reheating due to tidal dissipation. We then investigate the possibility of subcritical core accretion as envisioned for Uranus and Neptune. We show that a massive core surrounded by an envelope in hydrostatic equilibrium with the gaseous disk may indeed grow beyond $30M_{\oplus}$ provided the core accretion rate remains larger than $\sim 2 \times 10^{-5}M_{\oplus} \text{ yr}^{-1}$. However, we find the subcritical accretion scenario is very unlikely in the case of HD149026b for at least two reasons: (i) Subcritical planets are such that the ratio of their core mass to their total mass is above ~ 0.7 , in contradiction with constraints for all but the most extreme interior models of HD149026b; (ii) High accretion rates and large isolation mass required for the formation of a subcritical $> 35M_{\oplus}$ core are possible only at specific orbital distances in a disk with a surface density of dust equal to at least 10 times that of the minimum mass solar nebula. This value climbs to 30 when considering a $50M_{\oplus}$ core. These facts point toward two main routes for the formation of this planet: (i) Gas accretion that is limited by a slow viscous inflow of gas in an evaporating disk; (ii) A significant modification of the composition of the planet after gas accretion has stopped. These two routes are not mutually exclusive. Illustrating the second route, we show that for a wide range of impact parameters, giant impacts lead to a loss of the gas component of the planet and thus may lead to

planets that are highly enriched in heavy elements. Alternatively, the planet may be supplied with heavy elements by planetesimals by secular perturbations. Both in the giant impact and the secular perturbation scenarios, we expect an outer giant planet to be present. Observational studies by imaging, astrometry and long term interferometry of this system are needed to better narrow down the ensemble of possibilities.

Subject headings: planetary systems: formation

1. INTRODUCTION

The combined detection of extrasolar planets by radial velocimetry and transit photometry provides unique information by the measurement of both their mass and radius. Further spectroscopic studies of the system in and off transit can then even inform us on chemical species in the planet’s atmosphere, its possible evaporation, global atmospheric temperature, possible presence of winds, etc.

Nine transiting extrasolar planets have been discovered so far (see www.obspm.fr/planets). Eight of them have radii of 1.0–1.3 Jupiter’s radius (R_J), but one stands out: HD149026b has a radius of only $0.73 \pm 0.03R_J$ for a mass of 0.36 ± 0.03 Jupiter’s mass ($= 110 \pm 10M_{\oplus}$) and an orbital distance of 0.042 AU (Sato et al. 2005; Charbonneau et al. 2006). The parent star is believed to be $1.3M_{\odot}$, and is metal-rich with $[Fe/H] = 0.36 \pm 0.05$. Contrary to the other transiting extrasolar planets, believed to be mainly formed with hydrogen and helium (Burrows et al. 2000; Bodenheimer et al. 2001; Guillot & Showman 2002; Laughlin et al. 2005; Guillot 2005; Baraffe et al. 2005), HD149026b is *clearly* made of a significant fraction of heavy elements.

Indeed, based on evolution models, Sato et al. (2005) and then Fortney et al. (2006) have shown the planet has a huge rock/ice core of $\sim 70M_{\oplus}$. As noted by Sato et al. (2005), such a big core points toward formation of the planet in the core accretion scenario (e.g., Mizuno 1980; Bodenheimer & Pollack 1986), rather than in the disk instability scenario (e.g., Boss 1997). However, HD149026b may even challenge the core accretion scenario, because the core mass is far larger than that of Jupiter or Saturn, and the “canonical” critical core mass as derived by Mizuno (1980) is around $10M_{\oplus}$.

The purpose of this paper is to constrain the structure of HD149026b, to examine how the planet may have formed based on these constraints, and, hopefully, to stimulate further studies of the formation of close-in giant planets. In section 2, we attempt to constrain the structure of HD149026b based on various evolution models. In section 3, we then examine whether these constraints are compatible with the properties of growing protoplanetary cores embedded in a gaseous circumstellar disk. On these bases, various possibilities for the formation of this planet are explored in section 4. Section 5 summarizes the results and proposes two possible formation scenarios that account for the properties of HD149026b.

2. PRESENT STRUCTURE: HOW MUCH HEAVY ELEMENTS?

As already evident from the measurements and from previous models of the evolution of the planet (Sato et al. 2005; Fortney et al. 2006), HD149026b is surprisingly small, and should possess either a big core or a large amount of heavy elements in its interior. In this work, we attempt to constrain the core mass by using a variety of evolutionary models beyond those explored by Sato et al. and Fortney et al. In doing so, we will show that HD149026b indeed contains a significant amount of heavy elements, in apparent contradiction with current models of the formation of giant planets.

2.1. Standard Models

The evolution of a giant planet is essentially governed by a Kelvin-Helmholtz cooling and contraction similar to a stellar pre-main sequence evolution but slightly modified by degeneracy effects, and by the intense stellar irradiation that slows the cooling through the growth of a deep radiative region that can extend to kbar levels (Guillot et al. 1996; Guillot 2005).

The level of the irradiation received by the planet is calculated from the observations by Sato et al. (2005): We adopt values of the stellar radius ($R_* = 1.45 R_\odot$) and temperature ($T_* = 6150$ K) and the orbital distance of 0.046 AU to derive zero-albedo equilibrium temperature $T_{\text{eq}}^* = 1740$ K. We use this value as a minimum for the atmospheric temperature at the 1 bar level (the corresponding temperature found by Fortney et al. (2006) is between 2000 and 2200 K, and using the model of Iro, Bézard, & Guillot (2005), we find a value of 1980 K). We use the 1 bar level as outer boundary condition for the evolution models (see Guillot 2005).

Standard models are calculated on the basis of structure consisting of a central rock/ice core and of an envelope of solar composition, and further assuming that the planet has either formed *in situ* or moved rapidly to its present location, so that throughout its evolution it has received a constant stellar heat flux to slow its cooling.

For the core, we use the equations of state for “rocks” and “ices” obtained by Hubbard & Marley (1989). For the envelope, we use the H-He EOS from Saumon, Chabrier, & Van Horn (1995). The structure of the core with Hubbard & Marley (1989)’s EOS is independent of its temperature, but this simplification is reasonable because it has much smaller effects than changes in the (unknown) core composition. Although it has little effect on the models, we assume that the core luminosity is due both to radioactive decay (with $l_{\text{chondritic}} \approx 10^{20} \text{ erg s}^{-1} M_\oplus^{-1}$) and cooling (assuming that in the core the temperature is uniform and the specific heat is $c_v \approx 10^7 \text{ erg g}^{-1} \text{ K}^{-1}$). Internal opacities are calculated from Rosseland opacity tables provided by Allard et al. (2001).

The calculations are made for various core masses and core compositions and compared to the observational constraints in Fig. 1. As discussed by Sato et al. (2005) and by Fortney et al. (2006), the small planetary radius implies that it contains a large fraction of its mass in heavy elements.

Difference in composition of the core—whether these heavy elements are mostly “ices” (a mixture of water, ammonia and methane in their [unknown] high pressure, relatively high temperature form) or “rocks” (a mixture of refractory materials including mostly silicates)—affects the radius of the planet by 10 to 20%. For comparison, the interiors of Uranus and Neptune are consistent with being mostly made of “ices” (e.g., Podolak, Podolak, & Marley 2000). Figure 1 thus confirms the need for a substantial amount of heavy elements in HD149026b when adopting a standard evolution scenario. Quantitatively, this implies core masses between 41 and 83 M_{\oplus} in good agreement with Sato et al. (2005) and Fortney et al. (2006). In particular, the latter yields values between 60 and 93 M_{\oplus} . The difference is due to the fact that in order to constrain more strictly the minimum mass of heavy elements present in the planet, we used a low value of the atmospheric temperature.

2.2. The Cold Storage Hypothesis

We now investigate the hypothesis that the planet may have cooled far from its parent star before suddenly being sent into the presently observed 0.046 AU orbit. The reason for this sudden event is to be determined, but could be due to dynamical planet-planet interactions (see section 4.1.2). In terms of evolution, the planet is allowed to cool more rapidly during the time-period when it is far from the parent star. The sudden inward migration indeed yield an expansion of the planet but it may be limited to the outer layers and thus be relatively small (Burrows et al. 2000). We want to investigate whether the present mass and radius are compatible with a relatively small core.

We thus calculate evolution models similar to those in the previous section, but using $T_{\text{eq}} = 100$ K and an atmospheric model based on simplified radiative transfer calculations of an isolated atmosphere (see Saumon et al. 1996; Guillot 2005). Based on these calculations, we obtain generally a much faster contraction of the planet; a less than 30 M_{\oplus} core can account for the observed radius. However, we have to include reheating of the outer shell of the envelope. This shell is approximatively defined by the region whose temperature is lower than the new equilibrium temperature, 1740 K. Based on our calculations, this corresponds to a pressure level of ~ 10 kbar.

A simple estimation of the reheating timescale of the outer shell suggests that we have to include this effect. Using equations of radiative diffusion and energy conservation, we estimate that the reheating timescale of a layer of pressure P , temperature T , opacity κ and heat capacity c_p is to first order independent of its initial temperature and equal to:

$$\tau_{\text{rad}} \approx \frac{3c_p \kappa P^2}{4ac g^2 T^3}, \quad (1)$$

where a is the radiation density constant, c the speed of light, and g the planet’s gravity (assumed uniform). This expression is consistent with direct simulations by Iro, Bézard, & Guillot (2005). This timescale is about 10^8 years for $\kappa \approx 1 \text{ cm}^2 \text{ g}^{-1}$, $P \approx 10$ kbar, $g \approx 1550 \text{ cm s}^{-2}$, $T \approx 2000$ K and $c_p \approx 8 \times 10^7 \text{ erg g}^{-1} \text{ K}^{-1}$, which implies that the reheating is relatively fast and should involve most

of the shell that we defined.

However, the expansion due to the reheating is relatively small. The P^2 dependence ensures that most of this outer shell will be affected, and it will expand by a radius estimated to be:

$$\Delta R \approx H_p \Delta \ln P, \quad (2)$$

where $H_p \approx \mathcal{R}T/\mu g$ is the new pressure scale height and $\Delta \ln P$ measures the depth of the expanding shells in pressure units. Based on our simulations, a rough estimate is that the planet should expand by $\sim 4 \times 10^8$ cm ($= 0.06 R_J$) when considering levels between 10 kbar and 1 bar.

Note that this estimate does not include factors such as global reheating due to tidal dissipation caused by the necessary circularization of the planet’s spin and eccentricity. If such dissipation occurs sufficiently deep in the planet, this will lead to an expansion of the planet’s deeper layers that could completely erase the planet’s cold evolution phase (see Guillot 2005, and references therein). Thus, this very possibility that a planet can contract more efficiently far away from the star and then be brought in with little consequence on its radius is very much in question. We choose however to consider it because it gives a sense of the robustness of the conclusion that HD149026b contains a large fraction of heavy elements.

Table 1: Derived constraints on HD149026b’s composition. M_{HHe} and M_Z are masses of H/He and heavy elements, and $M_p = M_{\text{HHe}} + M_Z$ is total planetary mass.

	M_Z (M_\oplus)	M_{HHe} (M_\oplus)	M_Z/M_p
<i>In situ evolution</i>			
ices	50 – 83	27 – 54	0.52–0.72
rocks	41 – 69	38 – 64	0.43–0.60
<i>Cold storage scenario</i>			
ices	37 – 77	34 – 66	0.39–0.67
rocks	33 – 61	46 – 76	0.33–0.53
<i>Total</i>			
	33 – 83	27 – 76	0.33–0.72

Adding ΔR ($\sim 4 \times 10^8$ cm) to the radius obtained by the evolution calculation of the isolated planet (not including the global reheating), we derive masses of heavy elements that reproduce the observed radius and show these in Table 1. Even in the case of a long storage ($\gtrsim 10^8$ years) of the planet in a cold environment (corresponding to more than 10 AU), a large amount of heavy elements (strictly more than $33 M_\oplus$) is required to reproduce the observed radius of HD149026b.

2.3. Heavy Elements: In the Core or in the Envelope?

We have thus far assumed all heavy elements to lie within a central core. In order to see how the results are dependent on this assumption, we compare our previous model with a $60 M_{\oplus}$ ice core to a similar model with a $30 M_{\oplus}$ ice core and an envelope which is enriched by $30 M_{\oplus}$ of ices. For the ices in the envelope, we use the EOS described by Saumon & Guillot (2004).

Figure 2 shows the results of the calculations in the two cases: (i) with unchanged opacities (i.e., as calculated for a solar-composition mixture) and (ii) with 30 times larger opacities to mimic the effect of the enrichment of heavy elements in the envelope. Basically, when using an unchanged opacity table (the dotted line), there is very little difference between a planet that has all its heavy elements in the core and a planet that has them mixed throughout its envelope. However, large differences arise when the opacities are affected proportionally to the amount of heavy elements that are mixed (the dashed line). In that case, the cooling and contraction timescale, which is dominated by radiative transport in the outer radiative zone, becomes long, and prevents the rapid contraction of the planet.

These results confirm again that our estimates of the amount of heavy elements in HD149026b are lower limits and that the planet indeed must contain a significant amount of heavy elements. If most of the heavy elements are located below the radiative zone, which is not unlikely, then we expect our constraints to be relatively accurate. On the other hand, if the material is mixed in the outer radiative zone, we expect that its interior contains more heavy elements by up to $\sim 20 M_{\oplus}$ than calculated here.

2.4. Impact of the Various Parameters

We have used a rather simplified approach for the calculations of the interior structure. On the other hand, reality is without doubt more complex. However, this should not affect significantly the global constraints that are derived in Table 1. First, the two extreme compositions used for the heavy elements (“ices” and “rocks”) ensure that most variations due to improved EOS, for example, are likely to fall in between the range of values that are considered.

Our external boundary condition is extremely simplified. Although it agrees with more detailed atmospheric models, one has to account for the fact that the atmospheric temperatures may be higher, in particular if the atmosphere is itself enriched in heavy elements (see Fortney et al. 2006). A higher atmospheric temperature leads to a slightly larger radius, everything else being the same. However, given the decrease of the opacity with increasing temperature in that regime, the radius increase is very limited.

Other factors point toward a slightly larger amount of heavy elements than calculated here: (i) as discussed, the likely increase of the opacities in an enriched envelope; (ii) the presence of any other energy source such as the one that is required to reproduce the radius of HD209458b; (iii)

thermally-dependent EOS for the core. Again, given that the core mass is already quite large, we expect these factors not to change the masses of heavy elements that are inferred above.

3. A SUBCRITICAL CORE ACCRETION SCENARIO?

The structure of HD149026b as derived in the previous section is certainly puzzling: It contains as much hydrogen and helium as Saturn, but at least twice as much heavy elements. In other words, the ratio of heavy elements to hydrogen and helium is intermediate between those of Saturn and Uranus/Neptune. In the core accretion scenario, when core mass exceeds a critical value (called the *critical core mass*), the Kelvin-Helmholtz contraction of the envelope takes place, resulting in substantial disk-gas accretion onto the planet (e.g., Mizuno 1980; Bodenheimer & Pollack 1986). A widespread idea is that Jupiter and Saturn experienced the substantial gas accretion beyond the critical core mass, while the cores of Uranus and Neptune remained subcritical because of progressive accretion of planetesimals until the gaseous circumstellar disk disappeared (Pollack et al. 1996). In this section, we investigate whether HD149026b may have formed in a way similar to what envisioned for Uranus and Neptune.

3.1. Critical Core Mass and Gas Accretion Rate

Figure 3 shows the critical core mass ($M_{c,\text{crit}}$) as a function of core accretion rate for several different choices of distance from the parent star and local density of disk gas. In the numerical simulations we have used the H-He EOS from Saumon et al. (1995), the grain opacity from Pollack, McKay, & Christofferson (1985), and the gas opacity from Alexander & Ferguson (1994). The integration method is basically the same as that of Ikoma et al. (2000) who used simpler forms of EOS and gas and grain opacities.

The input physics used here is somewhat different from that used in section 2. First we include grain opacity that was not included in the simulations in section 2, because an accreting envelope contains low temperature parts in which grain opacity is dominant, unlike the fully-formed planet ($T \geq 1700$ K). Although the fully-formed planet also contains such low temperature parts in the cold storage model, the planet is almost fully convective. Second the gas opacity used in this simulation is different from that used in the previous section. This difference has little influence on the results obtained in this section, because most of the part of the envelope where gas opacity is dominant relative to grain opacity is convective. Finally, although constant core density is assumed here, the critical core mass is known to be insensitive to core density (Mizuno, Nakazawa, & Hayashi 1978).

Figure 3 shows a large subcritical core can be formed if core accretion rate is high. High core accretion rates stabilize the envelope, yielding progressively larger critical core masses (Ikoma et al. 2000). This, however, remains true up to a point for which the envelope becomes fully convective;

the structure of a fully convective envelope is almost adiabatic and thus independent of energy flux supplied by incoming planetesimals (i.e., core accretion rate). At that point, the critical core mass reaches its maximum value. In this case, this *maximal* critical core mass depends on the local disk conditions (i.e., the local density and temperature of disk gas and the distance from the parent star) (Wuchterl 1993; Ikoma, Emori, & Nakazawa 2001). In the minimum-mass solar nebula (MSN) proposed by Hayashi (1981), the entropy of the disk gas decreases as the distance to the parent star decreases. That is why the critical core mass is smaller at locations closer to the parent star: In a denser gas disk, the critical core mass is smaller for the same reason (Ikoma et al. 2001). As a result, formation of a large subcritical core of 50–80 M_{\oplus} requires not only high core accretion rate, but also a location not too close to its parent star and not too massive gaseous disk.

Although a large core of 50–80 M_{\oplus} can, in principle, be formed by subcritical growth as shown above, the ratio of the critical core mass to the corresponding total (core + envelope) mass suggests that the core mass of HD149026b was likely to be supercritical. Figure 4 shows the ratio of core mass to planetary total mass as a function of core mass (normalized by the critical core mass) for three different sets of core accretion rate and distance from the parent star. This ratio is found to be rather insensitive to values of the parameters; it is always ~ 0.7 at the critical core mass. The evolution model of HD149026b obtained in section 2 shows that the current ratio of core mass to planetary mass is smaller in most cases (see Table 1). Although there are a few cases where the current ratio is as large as ~ 0.7 , the probability of the formation of such planets seems to be low. From Fig. 4 we also find the duration during which the ratio of core mass to planetary mass is around ~ 0.7 is quite short in the total core formation time. It follows from this consideration that HD149026b is likely to have experienced disk-gas accretion due to the Kelvin-Helmholtz contraction of the envelope.

The rate of the gas accretion determined by the Kelvin-Helmholtz contraction of the envelope beyond the critical core mass—the gas accretion is hereafter called the KH gas accretion—depends strongly on the critical core mass. Figure 5 shows the typical timescale (τ_g) for the KH gas accretion defined by

$$\tau_g = C \frac{GM_{c,\text{crit}}M_{e,\text{crit}}}{R_{\text{conv}}L}, \quad (3)$$

where G is the gravitational constant, $M_{c,\text{crit}}$ is the critical core mass, $M_{e,\text{crit}}$ is the corresponding envelope mass, R_{conv} is the outer radius of the inner convective region, and L is the luminosity (Ikoma et al. 2000). The numerical factor, C , is chosen to be 3/2 based on the numerical simulations by Ikoma & Genda (2006). In cases where core accretion is suddenly stopped (corresponding to core isolation; see below), C should be 1/3 (Ikoma & Genda 2006). On this timescale the envelope mass increases by a factor of e . The timescale for the KH gas accretion is approximately expressed by

$$\tau_g \sim 5 \times 10^{10} \left(\frac{M_{c,\text{crit}}}{M_{\oplus}} \right)^{-3.5} \text{ years} \quad (4)$$

in this range¹. This relation implies that if the core mass is small, the timescale of the KH gas accretion is much longer than the disk lifetime ($\sim 10^6$ - 10^7 years).

For discussion in section 3.2, we have also drawn lines representing the time for formation of a critical core with constant core accretion rate,

$$\tau_{c,\text{acc,crit}} = \frac{M_c}{\dot{M}_c} \Big|_{M_c=M_{c,\text{crit}}}, \quad (5)$$

for three different sets of the parameters.

3.2. Subcritical Core Accretion

We examine the subcritical core accretion to know how large core can be formed before the onset of the KH gas accretion. Core mass is limited by the isolation mass that is determined by the total mass of solid components in the core’s feeding zone, unless planetesimals are supplied from outside the feeding zone by migration of planetesimals or the core itself. Merging between the isolated cores is not likely until disk gas is severely depleted (Iwasaki et al. 2002; Kominami & Ida 2002), because the eccentricity damping due to disk-planet interaction (Artymowicz 1993; Ward 1993) is too strong to allow orbital crossing of the isolated cores. The core isolation mass is thus given by (Ida & Lin 2004a)

$$M_{c,\text{iso}} \simeq 0.16 f_d^{3/2} \eta_{\text{ice}}^{3/2} \left(\frac{a}{1\text{AU}} \right)^{3/4} \left(\frac{M_*}{M_\odot} \right)^{-1/2} M_\oplus, \quad (6)$$

where a is semimajor axis of the core. The scaling factor f_g and f_d express enhancement of disk surface density of gas (Σ) and dust (σ) components relative to those of MSN, defined by

$$\begin{aligned} \Sigma &= 2400 f_g \left(\frac{a}{1\text{AU}} \right)^{-3/2} \text{g/cm}^2 \\ \sigma &= 10 f_d \eta_{\text{ice}} \left(\frac{a}{1\text{AU}} \right)^{-3/2} \text{g/cm}^2. \end{aligned} \quad (7)$$

In the solar metallicity cases, the values of these factors may have a range between 0.1 and 10 (Ida & Lin 2004a). For metal-rich disks, the range of f_d may shift to larger values by a factor of $10^{[\text{Fe}/\text{H}]}$, while that of f_g does not change (Ida & Lin 2004b). η_{ice} expresses an enhancement of disk surface density due to ice condensation, which is 3–4 beyond an ice line at ~ 3 AU. Equation (6) shows large cores form at large a , in particular beyond the ice line, in disks with large f_d . As seen from Fig. 3, smaller core accretion rate yields smaller critical core mass, which implies core isolation triggers the KH gas accretion. For a core of M_c not to be isolated, that is, $M_c < M_{c,\text{iso}}$,

$$f_d > 30 \left(\frac{M_c}{30M_\oplus} \right)^{2/3} \eta_{\text{ice}}^{-1} \left(\frac{a}{1\text{AU}} \right)^{-1/2} \left(\frac{M_*}{M_\odot} \right)^{1/3}. \quad (8)$$

¹The form of equation (4) is different from that of equation (19) of Ikoma et al. (2000). The difference comes mainly from the difference in grain opacity (see Ikoma & Genda 2006, for the detailed discussion).

Next, we consider the condition for a core to avoid the KH gas accretion until its isolation. Figure 3 shows that $M_{c,\text{crit}}$ is expressed approximately by

$$M_{c,\text{crit}} \simeq 10 \left(\frac{\dot{M}_c}{10^{-7} M_{\oplus}/\text{yr}} \right)^{0.2} M_{\oplus}, \quad (9)$$

except for fully convective cases. Note that consideration of fully convective cases does not change our conclusion (see below). The condition for a core to avoid the KH gas accretion is $M_c < M_{c,\text{crit}}$. Using $\tau_{c,\text{acc}} \equiv M_c/\dot{M}_c$ and Eq. (9), this condition is rewritten by (see Fig. 5)

$$\tau_{c,\text{acc}} < \tau_{c,\text{acc,crit}} \simeq 1 \times 10^6 \left(\frac{M_c}{30M_{\oplus}} \right)^{-4} \text{ years}. \quad (10)$$

For cores of 30 , 45 and $70M_{\oplus}$, $\tau_{c,\text{acc}}$ must be shorter than 1×10^6 years, 2×10^5 years, and 3×10^4 years, respectively. The core growth timescale due to planetesimal accretion is given by (Ida & Lin 2004a)

$$\tau_{c,\text{acc}} \simeq 9.3 \times 10^5 f_d^{-1} f_g^{-2/5} \eta_{\text{ice}}^{-1} \left(\frac{a}{1\text{AU}} \right)^{27/10} \left(\frac{M_c}{30M_{\oplus}} \right)^{1/3} \left(\frac{M_*}{M_{\odot}} \right)^{-1/6} \left(\frac{m}{10^{21}\text{g}} \right)^{2/15} \text{ years}, \quad (11)$$

where m is the mass of a planetesimal. The dependence on f_g appears because damping of velocity dispersion of planetesimals due to aerodynamical drag is taken into account. Substituting Eq. (11) into Eq. (10), we have

$$f_d > 0.95 \left(\frac{M_c}{30M_{\oplus}} \right)^{65/21} \left(\frac{f_d}{f_g} \right)^{2/7} \eta_{\text{ice}}^{-5/7} \left(\frac{a}{1\text{AU}} \right)^{27/14} \left(\frac{M_*}{M_{\odot}} \right)^{-5/42} \left(\frac{m}{10^{21}\text{g}} \right)^{2/21}. \quad (12)$$

This inequality indicates that large f_d is needed to keep core accretion rate high enough to avoid the KH gas accretion.

For subcritical core accretion, both Eqs. (8) and (12) must be satisfied. For $M_* = 1.3M_{\odot}$ and $[\text{Fe}/\text{H}]=0.36$ ($f_d/f_g = 2.3$), which correspond to HD149026, the conditions are plotted in Fig. 6. Subcritical core accretion could be possible far from the parent star in relatively massive disks for $30M_{\oplus}$ cores. However, for 45 and $70M_{\oplus}$ cores, extremely massive or extremely metal-rich disks with $f_d > 30-50$ are required. Even for those large values of f_d , since the critical core mass reaches its maximal value in cases of high core accretion rate, subcritical formation of 45 and $70 M_{\oplus}$ is impossible in some cases (see Fig. 3). Although formation of a $30M_{\oplus}$ core may not be very difficult in relatively metal-rich disks, $30M_{\oplus}$ is the lowest estimated value for M_Z of HD149026b in the cold storage model; $50-80M_{\oplus}$ is most likely. Therefore, heavy elements must be supplied after substantial accretion of the envelope. This issue is discussed in section 4.1.

4. SEVERAL POSSIBILITIES FOR THE FORMATION OF HD149026b

The investigations in sections 2 and 3 have revealed that we have to explain at least three properties of HD149026b: its small orbital radius, its high metallicity, and its moderate amount of hydrogen and helium.

A possible scenario that explains the proximity of the planet to its parent star is the *in situ* formation or migration of the planet. The *in situ* formation is however unlikely, because the core isolation mass is so small at ~ 0.04 AU (see eq. [6]) that the planet can get only a tiny amount of hydrogen/helium within the disk lifetime because of too long timescale for the KH gas accretion (see eq. [4]).

Section 3.2 has shown cores of $\gtrsim 30M_{\oplus}$ can form only far from the parent star in reasonably massive and/or metal-rich disks. Except for the cold storage model (section 2.2), residual heavy elements of $20\text{--}50M_{\oplus}$ must be supplied to the planet. In section 4.1, we examine two possible scenarios; supply of heavy elements (planetesimals or another planet) during gas accretion (§ 4.1.1) and after disk gas depletion (§ 4.1.2). To account for the moderate amount of hydrogen and helium of HD149026b, we examine limited supply of disk gas (§ 4.2.1) and loss of the envelope gas (§ 4.2.2).

4.1. Supply of Heavy Elements

4.1.1. During gas accretion

First we briefly discuss the possibility that the large amount of heavy elements in HD149026b were supplied *during* substantial accretion of the envelope that happened far from the parent star. An increase in the planet’s mass due to gas accretion expands its feeding zone. If the planet can efficiently capture the planetesimals in the feeding zone, supply of heavy elements during gas accretion is possible (Pollack et al. 1996; Alibert, Mordasini, & Benz 2004). However, the cross section of gravitational scattering is much larger than that of collision in outer regions. Most planetesimals are thus scattered before accretion onto the planet. The gravitational scattering combined with eccentricity damping by disk-gas drag ends up opening a gap in the planetesimal disk: This phenomenon is called “shepherding” (e.g., Tanaka & Ida 1997)². Although fast migration or growth of the planet can avoid the gap opening, unrealistically fast migration or growth may be required for a Saturn-mass planet to avoid the gap opening (Tanaka & Ida 1999; Ida et al. 2000). Thus, supply of a large amount of planetesimals may be unlikely to happen during gas accretion.

However, much more detailed studies are needed for this possibility. If the shepherding completely prevented the planetesimal accretion throughout the gas accretion phase, the well-known enrichment of heavy elements in the envelopes of Jupiter and Saturn would be unable to be accounted for. A possibility is accretion of small fragments. Small fragments are produced by disruptive collisions of planetesimals in the vicinity of a large core (Inaba, Wetherill, & Ikoma 2003). Since atmospheric-gas drag is strong for the fragments, they are accreted onto the core (Inaba & Ikoma 2003). Because these studies are limited to the subcritical core case, we need to extend the calculation to the case of supercritical cores, in which the planet mass rapidly increases and

²The shepherding by isolated mean-motion resonances is called “resonant trapping” (e.g., Weidenschilling & Davis 1985; Kary, Lissauer, & Greenzweig 1993).

non-uniformity of disk gas is pronounced.

4.1.2. After disk gas depletion

We next explore the possibility of enrichment of heavy elements in HD149026b (i.e., bombardment of another planet or planetesimals) *after* substantial accretion of the envelope.

If the late bombardment happened, it is likely to have occurred after the planet migrated to its current location: The close-in planet collided with another planet(s) or planetesimals that had been gravitationally scattered by an outer giant planet(s). At ~ 0.05 AU the planet’s Hill radius is only several times as large as its physical radius, while the former is much larger (by 100–1000) than the latter in outer regions ($\gtrsim 1$ AU). That means the ratio of collision to scattering cross sections is much larger at ~ 0.05 AU relative to in outer regions. The scattering cross section is further reduced by high speed encounter. The impact velocities (v_{imp}) of the scattered bodies in nearly parabolic orbits are as large as the local Keplerian velocity at ~ 0.05 AU, which is a few times larger than surface escape velocity of the inner Saturn-mass planet (v_{esc}). The collision cross section is, in general, larger than the scattering cross section for $v_{\text{imp}} > v_{\text{esc}}$. Note that the shepherding does not work for highly eccentric orbits.

To know how efficiently such scattered bodies collide with the close-in giant planet, we perform the following numerical simulation. We consider an inner planet of $0.5M_{\text{J}}$ in a circular orbit at 0.05 AU and a planetesimal (test particle) or another giant planet of $0.5M_{\text{J}}$ in a nearly parabolic orbit of $e \simeq 1$ and $i = 0.01$ with initial semimajor axis of $a = 1$ AU. For each initial pericenter distance (q), 100 cases with random angular distributions are numerically integrated by 4th order Hermite integrator for 100 Keplerian periods at 1 AU. Then, collision probability with the inner planet (P_{col}), that with the parent star (P_{col}^*), and ejection probability (P_{ejc}) are counted. The residual fraction, $1 - (P_{\text{col}} + P_{\text{col}}^* + P_{\text{ejc}})$, corresponds to the cases in which the planetesimal/planet is still orbiting after 100 Keplerian periods. We also did longer calculations and found that $P_{\text{col}}/P_{\text{ejc}}$ is similar, although individual absolute values of P_{col} and P_{ejc} increases. The results are insensitive to a as long as $a \gg 0.05$ AU, because velocity and specific angular momentum of the incoming planetesimal/planet are given by $v \simeq \sqrt{2GM_*/q}$ and $L \simeq \sqrt{2GM_*q}$ that are independent of initial semimajor axis a of incoming bodies.

Figure 7 shows the probabilities of the three outcomes of encounters between the inner planet and a planetesimal (panel a) or another giant planet (panel b). As shown in Fig. 7, when $0.01\text{AU} < q < 0.06\text{AU}$, the incoming bodies closely approach the inner planet. Although some fraction of them are ejected, the comparable fraction results in collision with the inner planet. In particular, $P_{\text{col}} > P_{\text{ejc}}$ in the planet-planet case (panel b), in which the ratio of geometrical cross section to Hill radius is larger than in the planet-planetesimal case (panel a). If q is smaller than or close to the parent star’s physical radius (which is 0.01 AU in the calculations here), most of the incoming bodies hit the parent star rather than collide with the inner planet. If $q > 0.06$ AU, they do not

closely encounter with the inner planet, so that both collision and ejection probabilities almost vanish ($P_{\text{col}}, P_{\text{ejc}} \ll 1$).

The results shown in Fig. 7 demonstrate that efficient supply of heavy elements to the inner giant planet requires a very limited range (close to unity) of eccentricities of the incoming bodies; for example, $0.94 < e < 0.99$ for $a = 1$ AU, since $q = a(1 - e)$. In the case of chaotic scattering by outer giant planets, the probability to acquire q in such a narrow range would be very small (e.g., Ford, Havlickova, & Rasio 2001). On the other hand, if the scattering comes from secular perturbation, e is increased secularly while a is kept constant. Accordingly, q decreases secularly, and the incoming bodies eventually collide with the inner planet.

For example, the following scenario is possible. More than three giant planets in addition to the inner one are formed in nearly circular orbits. They start orbit crossing on timescales longer than their formation timescales (Rasio & Ford 1996; Weidenschilling & Marzari 1996; Lin & Ida 1997; Marzari & Weidenschilling 2002). In many cases, one giant planet is ejected and the residual giant planets remain in stable eccentric orbits after the orbit crossing (Marzari & Weidenschilling 2002). In about 1/3 cases, q of a giant planet decreases secularly to $\lesssim 0.05$ AU due to the Kozai effect (Kozai 1962) during the orbit crossing (Nagasawa et al. 2006). This scenario requires formation of at least four giant planets.

4.2. Origin of the Small Amount of Hydrogen and Helium

4.2.1. Limited disk gas supply

Gas accretion onto a core can be truncated by gap opening or global depletion of disk gas. A gap may be formed, if both the viscous and thermal conditions are satisfied (e.g., Lin & Papaloizou 1985, 1993; Crida, Morbidelli, & Masset 2006). The former is that the torque exerted by the planet overwhelms viscous torque, and given by (Ida & Lin 2004a),

$$M_{\text{p}} > M_{\text{p,vis}} = 30 \left(\frac{\alpha}{10^{-3}} \right) \left(\frac{a}{1\text{AU}} \right)^{1/2} \left(\frac{M_{*}}{M_{\odot}} \right) M_{\oplus}, \quad (13)$$

where M_{p} is the planet mass and α is the parameter for the α -prescription for disk viscosity (Shakura & Sunyaev 1973). The latter condition is that the Hill radius becomes larger than disk scale height, and given by³ (Ida & Lin 2004a)

$$M_{\text{p}} > M_{\text{p,th}} = 400 \left(\frac{a}{1\text{AU}} \right)^{3/4} \left(\frac{M_{*}}{M_{\odot}} \right) M_{\oplus}, \quad (14)$$

assuming an optically thin disk in which $T = 280(a/1\text{AU})^{-1/2}$ K. Hence, the actual truncation condition may be the thermal condition and it is very unlikely that gas accretion is truncated by

³Here we assume the Hill radius ($r_{\text{H,c}}$) is equal to 1.5 times disk scale height (h), roughly taking into account late gas accretion with a reduced rate after $r_{\text{H,c}} = h$, following Ida & Lin (2004a).

the gap opening at $M_p \sim 110M_\oplus$ (which corresponds to HD149026b) far from the parent star, as long as a sufficient amount of disk gas remains. Furthermore, since the gap is replenished by viscous diffusion, gas accretion may not completely be truncated by the gap opening (D’Angelo, Kley, & Henning 2003).

If a sufficient amount of disk gas remains, one way to truncate gas accretion at relatively small planetary mass is that the planet migrates to the vicinity of its parent star before the planet accretes a large amount of gas. Both $M_{p,\text{vis}}$ and $M_{p,\text{th}}$ are small in the inner regions (Eqs. [13] and [14]). However, this is unlikely, even if type II migration occurs when $M_p \sim 30M_\oplus$. The timescale for the KH gas accretion $\lesssim 3 \times 10^4$ years for a core of $\gtrsim 30M_\oplus$ (Fig. 5), while the timescale for the migration is much longer ($\sim 10^6$ – 10^7 years). Furthermore, it is not clear if the gap opening can stop gas accretion completely.

If disk gas is globally depleted when M_c reaches $M_{c,\text{crit}}$, gas accretion onto the core can be limited by viscous diffusion of disk gas, not by the Kelvin-Helmholtz contraction of the envelope (e.g., Guillot & Hueso 2006). That could be possible to account for the small amount of H/He. However, whether such a small amount of disk gas can bring the planet to the vicinity of the parent star should be examined. If it does not work, different migration mechanism such as gravitational scattering during orbital crossing of giant planets is required.

4.2.2. Loss of envelope gas

Another way to explain the small amount of the H/He gas of HD149026b is loss of the envelope gas. There are three possibilities for loss of the envelope gas; photoevaporation driven by incident UV flux from the parent star, the Roche lobe overflow, and impact erosion by a collision with another gas giant planet.

Photoevaporation process for gas-rich planets is normally faster for smaller planetary masses, because less massive planets are more expanded and their envelope gas is more loosely bound (Baraffe et al. 2005). This means the envelope quickly disappears once the evaporation occurs, so that it should be relatively rare to observe a planet at a stage when a relatively small amount (30–60 M_\oplus) of envelope gas remains. However, this possibility is not excluded at present, because Z -rich planets such as HD149026b can be more compact and their envelope gas is not necessarily more loosely bound (e.g., Baraffe et al. 2006).

Envelope gas can also be lost by the Roche lobe overflow. When the Roche lobe is filled with the envelope gas, the gas overflows through the inner Lagrangian point to the inner disk. The Roche lobe overflow takes place if a planet is very close to its parent star because of inflation by stellar tidal heating as well as reduction of the Roche lobe (e.g., Trilling et al. 1998), and subsequent tidal inflation instability of the envelope (e.g., Gu, Lin, & Bodenheimer 2003). The spilled gas from the Roche lobe first goes to the inner disk and is eventually going to fall on the parent star by the gravitational interaction with the planet. At the same time, the planet gains angular momentum

as the counteraction and migrates outward. Because of the increase in the orbital radius, the evaporation process slows down. Thus a state of a 30–60 M_{\oplus} envelope could be possible. This possibility is, however, in question because it is unclear if sufficient angular momentum is lost.

Sato et al. (2005) suggested that collision between two giant planets could account for the internal structure of HD149026b. If cores with individual mass of $\sim 30M_{\oplus}$ are merged while significant amounts of their envelopes evaporate, a planet similar to HD149026b is formed. Here we examine if significant loss of the envelope gas occurs through SPH simulations of a collision between two giant planets.

High impact velocity is expected. Suppose that one giant planet orbits at 0.03–0.05 AU and another giant planet in a highly eccentric orbit is sent from an outer region (for the mechanism to send planets, see section 4.1.2). Since the impactor has high orbital eccentricity ($e \sim 1$), collision velocity is similar to local Keplerian velocity at 0.03–0.05 AU around a $1.3M_{\odot}$ star, 150–190 km/s. This velocity is 2–3 times as high as the two-body surface escape velocity. Since specific angular momentum of the impactor is given by $L = \sqrt{GM_*a(1-e^2)} \simeq \sqrt{2GM_*q}$, the impactor and the target have similar L . Hence, the semimajor axis of the merged planet would be similar to that of the target planet unless envelope evaporation changes specific angular momentum significantly.

Previous SPH simulations of a collision between Mars-size or Earth-size rocky planets (e.g., Canup 2004; Agnor & Asphaug 2004) show almost no loss of material occurs by a low-velocity impact (v_{imp}) of 1.0–1.5 times as high as the two-body surface escape velocity (v_{esc}) defined by $v_{\text{esc}}^2 = 2G(M_t + M_i)/(R_t + R_i)$, where M and R are the planetary mass and radius and subscriptions t and i represent the target and the impactor. Collisions with higher impact velocity lose larger amounts of material; for example, 40% of the total mass is lost when $v_{\text{imp}} \sim 2.5v_{\text{esc}}$ in their simulations. For gas giant planets, we will have qualitatively similar results, but can expect more significant loss of envelope gas because the envelope is less tightly bound compared to rocky planets.

In order to simulate the collision between two gas giant planets, we use a SPH method with the modified spline kernel function (Monaghan & Lattanzio 1985) and artificial viscosity (Monaghan & Gingold 1983). Our SPH simulation code was checked to reproduce the results of Agnor & Asphaug (2004) for Mars-size planets using the Tillotson EOS. In this paper, we assume that the gas giant planets are composed only of ideal gas with the adiabatic exponent of 2; this value reproduces the present structure of Jupiter. We consider two hydrostatically equilibrated planets (each being composed of about 30,000 SPH particles) with Jupiter’s mass and radius for initial conditions. We perform the simulations of head-on collisions with various impact velocities (1.0, 1.5, 2.0, 2.25, 2.5, and $3.0v_{\text{esc}}$). In our calculations, v_{esc} is 60 km/s. We calculate the gravitational force for each SPH particle using the special-purpose computer for gravitational N-body systems, GRAPE-6.

Figure 8 shows the mass fraction lost by collisions with various impact velocities. Higher impact velocity results in higher loss fraction. Almost no escape occurs for a low-velocity impact ($v_{\text{imp}} \sim v_{\text{esc}}$). When the impact velocity is higher than $2.5v_{\text{esc}}$, almost all SPH particles ($\sim 90\%$) are lost.

Although we are unable to know exactly the loss fraction of the core with our current simulation, we can estimate it approximately by tracking the motion of the SPH particles which are initially located in inner part of the planet. Figure 8 also shows the loss fractions of the inner parts that are initially located inside 1/2 and 1/4 of the planetary radius. The inner part of the planet tends to remain in the merged planet. For example, in the case of $2.0v_{\text{esc}}$, about 50% of materials is totally lost, but almost no escape occurs for the material inside of 1/4 initial radius. A head-on collision of two gas giant planets with $v_{\text{imp}} \sim 2\text{--}2.5v_{\text{esc}}$ possibly results in the considerable depletion of envelope and merging of core.

The strongest point of this model for envelope loss is that we need no additional process to supply heavy elements to the planet. The collision increases M_Z up to $\sim 60M_{\oplus}$ as well as decreases M_{HHe} ; as we showed in section 3.2, it is possible to form cores of $\sim 30M_{\oplus}$ by ordinary planetesimal accretion in relatively massive disks, in particular, metal-rich disks. However, the numerical simulations performed here is still preliminary. Since this mechanism may be promising, we should perform detailed simulations in the future.

4.3. Other Possibilities

Another possibility of formation of a metal-rich giant planet is the formation in a disk with originally high dust/gas ratio. In general, dust grains migrate inward in a gas disk to change the local dust/gas ratio (e.g., Stepinski & Valageas 1997). If the dust/gas ratio is enhanced in planet-forming regions at $\lesssim 10$ AU, the metal-enriched envelope could be formed without any planetesimal/planet supply. The high dust/gas ratio also makes possible planetesimal formation from dust through self-gravitational instability against Kelvin-Helmholtz instability (Youdin & Shu 2002) and avoids type-I migration of terrestrial planets (Kominami, Tanaka & Ida 2005). However, it is not clear if the dust/gas ratio can become large enough to account for M_Z of HD149026b.

In principle, it is possible for a $70M_{\oplus}$ core to form at ~ 0.05 AU through accretion of many Earth-size to Uranian-size cores that migrate close to the parent star. In the vicinity of the parent star, gas accretion should be truncated at a relatively small mass (see eq. [14]). We may need to carry out N-body simulations of the migrating protoplanets in order to examine whether they can pass through resonant trapping (or shepherding) to merge or not. However, we should keep in mind that incorporation of type-I migration without any conditions causes severe inconsistency with observed data of extrasolar planets and our Solar System. If we rely on type-I migration model, we need to clarify the condition for the occurrence of type-I migration at the same time.

5. SUMMARY AND CONCLUSIONS

The high density of the close-in extrasolar giant planet HD149026b recently discovered by Sato et al. (2005) challenges theories of planet formation. In this paper, we have attempted to derive

robust constraints on the planet’s composition and infer possible routes to explain its formation.

We have first simulated the evolution of HD149026b more extensively than previous workers (Sato et al. 2005; Fortney et al. 2006) and confirmed that the planet contains a substantial amount of heavy elements. Preferred values of the total mass of heavy elements are 50–80 M_{\oplus} (section 2.1), which is consistent with the previous calculations. We showed that the results are unchanged for heavy elements located in the central core, or distributed inside the envelope, provided they remain deeper than the external radiative zone. In the event of a significant enrichment of the outer layers, slightly higher values of heavy elements content are possible (section 2.3). In order to derive minimum values of the mass of heavy elements, we have explored the possibility that the planet was stored in a relatively cold environment for some time before migrating near to the planet. This strict minimum is $\sim 35M_{\oplus}$, but is regarded as unlikely because it requires a late migration and no reheating of the planet by tidal circulization (section 2.2).

We have then investigated the possibility of subcritical core accretion as envisioned for Uranus and Neptune to account for the small envelope mass as well as the large core mass. In principle a large core of 50–80 M_{\oplus} can be formed by subcritical core accretion. However we have found it very unlikely for at least two reasons: (i) A subcritical core accretion results in a ratio of the core mass to the total mass above ~ 0.7 (section 3.1), whereas our evolution calculations showed such a high ratio to be possible in a very limited range of parameters (see Table 1); (ii) The subcritical formation of a 50–80 M_{\oplus} core requires an extremely massive or metal-rich disk with dust surface density 30-50 times the values obtained for the minimum mass solar nebula (section 3.2). A reasonably massive and/or metal-rich disk can form cores of at most $\sim 30M_{\oplus}$ far from the parent star. Those facts require us to consider (i) the migration of the planet, (ii) the supply of heavy elements to the planet during or after the gas accretion phase, and (iii) a limited supply of disk gas or loss of the envelope gas to account for the properties of HD149026b.

In section 4.1, we have discussed how the heavy elements can be delivered to the planet during or after the gas accretion phase according to these scenarios. An efficient delivery during the gas accretion phase needs to be re-investigated in much more details, because the shepherding tends to prevent the planet from accreting planetesimals (section 4.1.1). On the other hand, scattering of planetesimals/planets by one or several outer giant planets was shown to lead to an efficient accretion by a close-in giant planet, and is a promising explanation for the formation of metal-rich planets (section 4.1.2).

The relatively small amount of hydrogen and helium present in HD149026b is also to be explained by the relatively slow formation of the planet in a low-density environment (section 4.2.1). Another possibility is related to erosion of the envelope during giant impacts. A reasonable impact velocity of 2–2.5 times the two-body surface escape velocity was found to result in a substantial loss of the envelope gas, while solid cores are probably merged (section 4.2.2).

In summary, we can propose at least two scenarios for the origin of HD149026b.

- A giant planet with a core of $\sim 30M_{\oplus}$ forms far from its parent star in a relatively massive and/or metal-rich disk. Then it moves to the vicinity of the parent star through type-II migration (Lin et al. 1996). In the outer regions additional more than three giant planets form, which may be likely in massive/metal-rich disks (Ida & Lin 2004a,b). They starts orbit crossing and the innermost one is temporally detached from the outer two. The perturbation from the outer two secularly pumps up the eccentricity of the innermost one (Nagasawa et al. 2006). The associated secular decrease of its pericenter distance results in collision with the close-in planet. The impactor also has a core of $\sim 30M_{\oplus}$. Their solid cores are merged to form a core of $\sim 60M_{\oplus}$, while envelope gas is severely eroded to $M_{\text{HHe}} \sim 50M_{\oplus}$. The orbital eccentricity of the merged body is damped by tidal interaction with the parent star.
- A $\sim 30M_{\oplus}$ core forms in an evaporating disk that was originally massive and/or metal rich. The core thus becomes supercritical, but the accretion of the envelope is limited by viscous diffusion in an evolved, extended gaseous disk (see Guillot & Hueso 2006). The planet subsequently accretes heavy elements through the delivery of planetesimals and/or planets, either because of migration due to interactions with the gas disk or to secular perturbations with a massive outer planet.

Above two scenarios are different from each other in that the former leaves at least one outer giant planet while the latter does not necessarily need any outer giant planets. Long-term radial velocity observations of HD149026b are thus needed to determine the presence of other planets in the system.

We thank the anonymous referee for fruitful comments. This research was supported by Ministry of Education, Culture, Sports, Science and Technology of Japan, Grant-in-Aid for Scientific Research on Priority Areas, “Development of Extra-solar Planetary Science”.

REFERENCES

- Agnor, C. & Asphaug, E. 2004, *ApJ*, 613, L157
- Allard, F., Hauschildt, P. H., Alexander, D. R., Tamanai, A., & Schweitzer, A. 2001, *ApJ*, 556, 357
- Alexander, D. R. & Ferguson, J. W. 1994, *ApJ*, 437, 879
- Alibert, Y., Mordasini, C., & Benz, W. 2004, *A&A*, 417, L25
- Artymowicz, P. 1993, *ApJ*, 419, 166
- Baraffe, I., et al. 2005, *A&A*, 436, L47
- Baraffe, I., Alibert, Y., Chabrier, G., & Benz, W. 2006, *A&A*, 450, 1221
- Bodenheimer, P., & Pollack, J. B. 1986, *Icarus*, 67, 391
- Bodenheimer, P., Lin, D. N. C., & Mardling, R. A. 2001, *ApJ*, 548, 466
- Boss, A. P. 1997, *Science*, 276, 1836
- Burrows, A., Guillot, T., Hubbard, W. B., Marley, M. S., Saumon, D., Lunine, J. I., & Sudarsky, D. 2000, *ApJ*, 534, L97
- Canup, R. M. 2004, *Icarus*, 168, 433
- Charbonneau, D., et al. 2006, *ApJ*, 636, 445
- Crida, A., Morbidelli, A., & Masset, F. 2006, *Icarus*, 181, 587
- D'Angelo, G., Kley, W., & Henning, T. 2003, *ApJ*, 586, 540
- Ford, E. B., Havlickova, M., & Rasio, F. A. 2001, *Icarus*, 150, 303
- Fortney, J. J., Saumon, D., Marley, M. S., Lodders, K., & Freedman, R. S. 2006, *ApJ*, in press (astro-ph/0507422)
- Guillot, T., Burrows, A., Hubbard, W.B., Lunine, J.I. & Saumon, D. 1996, *ApJ*, 459, L35
- Guillot, T. 2005, *AREPS*, 33, 493
- Guillot, T., & Hueso R. 2006, *MNRAS*, 367, L47
- Guillot, T., & Showman, A. P. 2002, *A&A*, 385, 156
- Gu, P-G, Lin, D. N. C., & Bodenheimer, P. 2003, *ApJ*, 588, 509
- Hayashi, C. 1981, *Prog. Theor. Phys. Suppl.*, 70, 35

- Hubbard, W. B., & Marley, M. S. 1989, *Icarus*, 78, 102
- Ida, S., Bryden, G., Lin, D. N. C., & Tanaka, H. 2000, *ApJ*, 534, 428
- Ida, S., & Lin, D. N. C. 2004a, *ApJ*, 604, 388
- Ida, S., & Lin, D. N. C. 2004b, *ApJ*, 616, 567
- Ikoma, M., Emori, H., & Nakazawa, K. 2001, *ApJ*, 553, 999
- Ikoma, M., & Genda, H. 2006, *ApJ*, in press
- Ikoma, M., Nakazawa, K., & Emori, H. 2000, *ApJ*, 537, 1013
- Inaba, S., & Ikoma, M. 2003, *A&A*, 410, 711
- Inaba, S., Wetherill, G. W., & Ikoma, M. 2003, *Icarus*, 166, 46
- Iro, N., Bézard, B., & Guillot, T. 2005, *A&A*, 436, 719
- Iwasaki, K., Emori, H., Nakazawa, K., & Tanaka, H. 2002, *PASJ*, 54, 471
- Kary, D. M., Lissauer, J. J., & Greenzweig, Y. 1993, *Icarus*106, 228
- Kominami, J., & Ida, S. 2002, *Icarus*, 157, 43
- Kominami, J., Tanaka, H., & Ida, S. 2006, *Icarus*, submitted
- Kozai, Y. 1962, *AJ*, 67, 591
- Laughlin, G., Wolf, A., Vanmunster, T., Bodenheimer, P., Fischer, D., Marcy, G., Butler, P., & Vogt, S. 2005, *ApJ*, 621, 1072
- Lin, D. N. C., Bodenheimer, P., & Richardson, D. 1996, *Nature*, 380, 606
- Lin, D. N. C., & Ida, S. 1997, *ApJ*, 477, 781
- Lin, D. N. C., & Papaloizou, J. C. B. 1985, *Protostars and Planets II*, ed. D. C. Black & M. S. Matthew (Tucson: Univ. of Arizona Press), 981
- Lin, D. N. C., & Papaloizou, J. C. B. 1993, in *Protostars and Planets III*, ed. E. H. Levy and J. I. Lunine (Tucson: Univ. of Arizona Press), 749
- Monaghan, J. J., & Gingold, R. A. 1983, *J. Comp. Phys.*, 52, 375
- Monaghan, J. J., & Lattanzio, J. C. 1985, *A&A*, 149, 135
- Marzari, F., & Weidenschilling, S. 2002, *Icarus*, 156, 570
- Mizuno, H. 1980, *Prog. Theor. Phys. Suppl.*, 64, 54

- Mizuno, H., Nakazawa, K., & Hayashi, C. 1978, *Prog. Theor. Phys.*, 60, 699
- Nagasawa, M., Bessho, T., Tanaka, H., & Ida, S., in preparation
- Podolak, M., Podolak, J. I., & Marley, M. S. 2000, *Planet. Space Sci.*, 48, 143
- Pollack, J. B., McKay, C. P., & Christofferson, B. M. 1985, *Icarus*, 64, 471
- Pollack, J. B., Hubickyj, O., Bodenheimer, P., Lissauer, J. J., Podolak, M., & Greenzweig, Y. 1996, *Icarus*, 124, 62
- Rasio, F. A., & Ford, E. B. 1996, *Science*, 274, 954
- Sato, B., et al. 2005, *ApJ*, 633, 465
- Saumon, D., Chabrier, G., & Van Horn, H. M. 1995, *ApJS*, 99, 713
- Saumon, D., & Guillot, T. 2004, *ApJ*, 609, 1170
- Saumon, D., Hubbard, W. B., Burrows, A., Guillot, T., Lunine, J. I., & Chabrier, G. 1996, *ApJ*, 460, 993
- Shakura, N. I., & Sunyaev, R. A. 1973, *A&A*, 24, 337
- Stepinski, T. F., & Valageas, P. 1997, *A&A*, 319, 1007
- Tanaka, H., & Ida, S. 1997, *Icarus*, 125, 302
- Tanaka, H., & Ida, S. 1999, *Icarus*, 139, 350
- Trilling, D. E., Benz, W., Guillot, T., Lunine, J. I., Hubbard, W. B., & Burrows, A. 1998, *ApJ*, 500, 428
- Ward, W. 1993, *Icarus*, 106, 274
- Weidenschilling, S. J., & Davis, D. R. 1985, *Icarus*, 62, 16
- Weidenschilling, S. J., & Marzari, F. 1996, *Nature*, 384, 619
- Wuchterl, G. 1993, *Icarus*, 106, 323
- Youdin, A. N., & Shu, F. H. 2002, *ApJ*, 580, 494

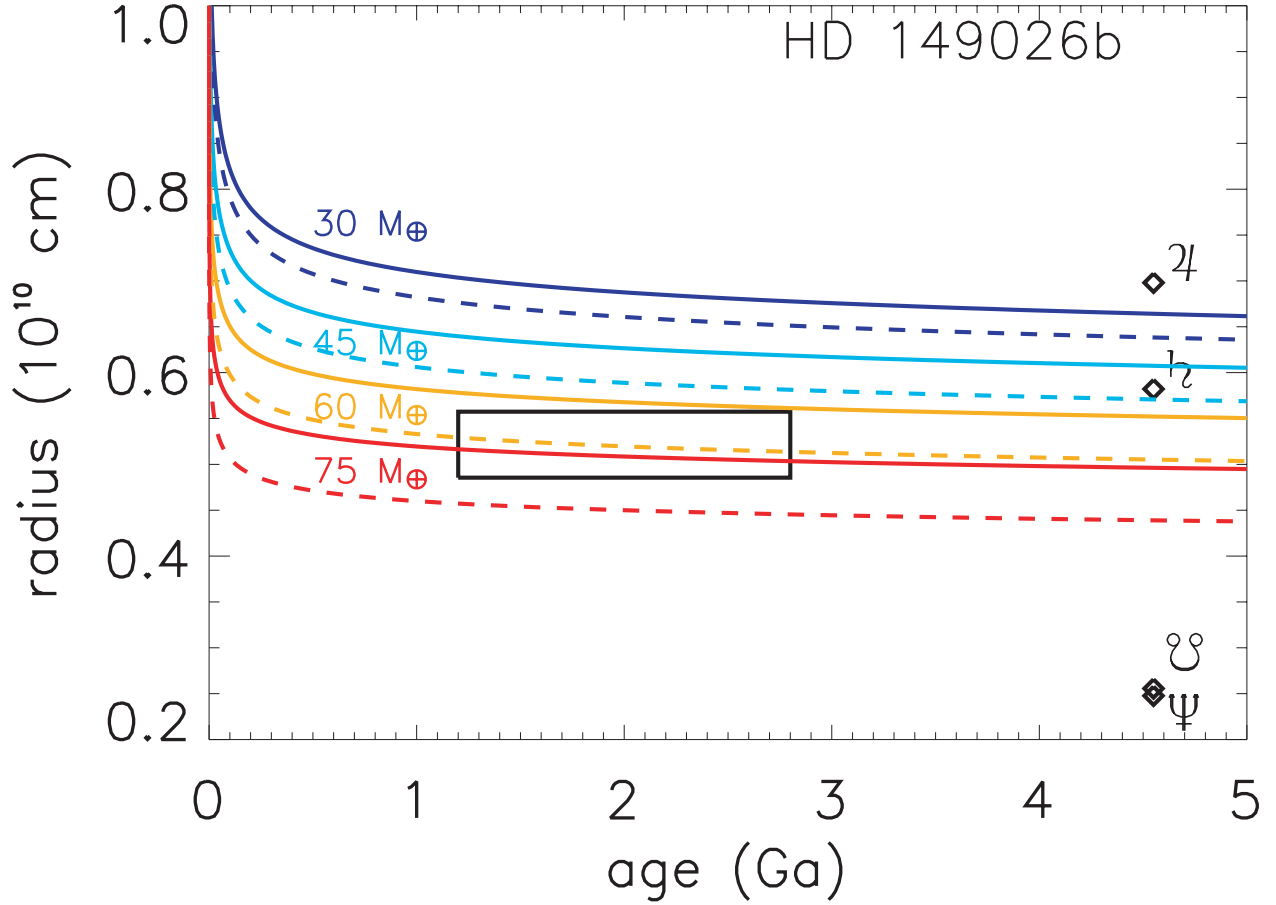


Fig. 1.— Evolution of the radius of a $0.36 M_J$ planet made of a central core of 30 to $75 M_{\oplus}$ and a gaseous envelope of solar composition. The planet is irradiated so that $T_{\text{eq}}^* = 1740$ K (see text). The core is assumed to be made of ices (plain lines) or rocks (dashed lines). The results are compared to the observational constraints on the age and radius of HD149026b (black box).

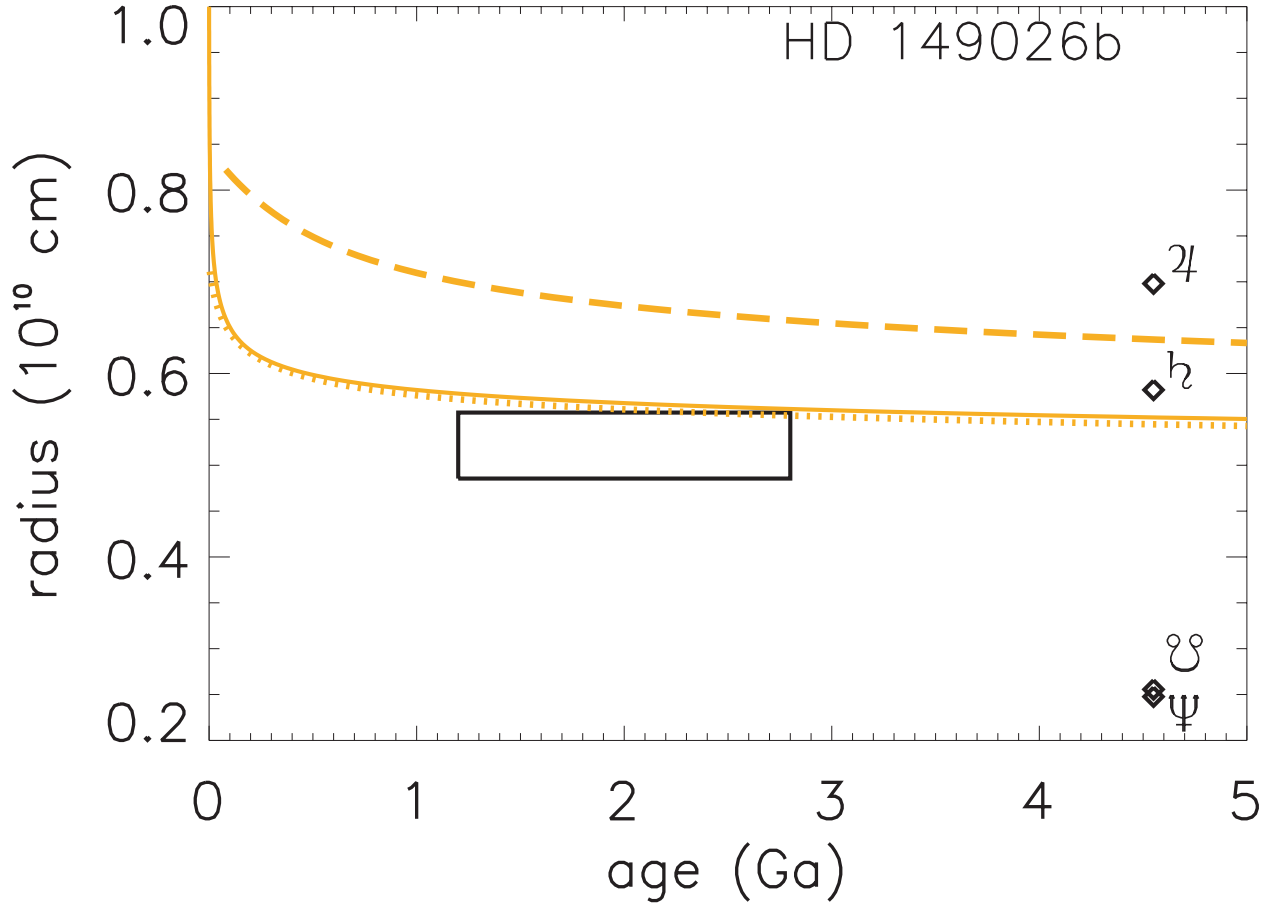


Fig. 2.— Evolution of the radius of a $0.36 M_J$ planet. The plain line corresponds to the case of a $60 M_\oplus$ ice core with a solar composition envelope shown in Fig. 1. The dotted line represents the result of the calculation with a $30 M_\oplus$ ice core and $30 M_\oplus$ of ices in the envelope; opacities were calculated for a solar-composition mixture. The dashed line is the same calculation, but with an opacity that is artificially increased by 30 to account for the presence of heavy elements in the envelope. The results are compared to the observational constraints on the age and radius of HD149026b (black box).

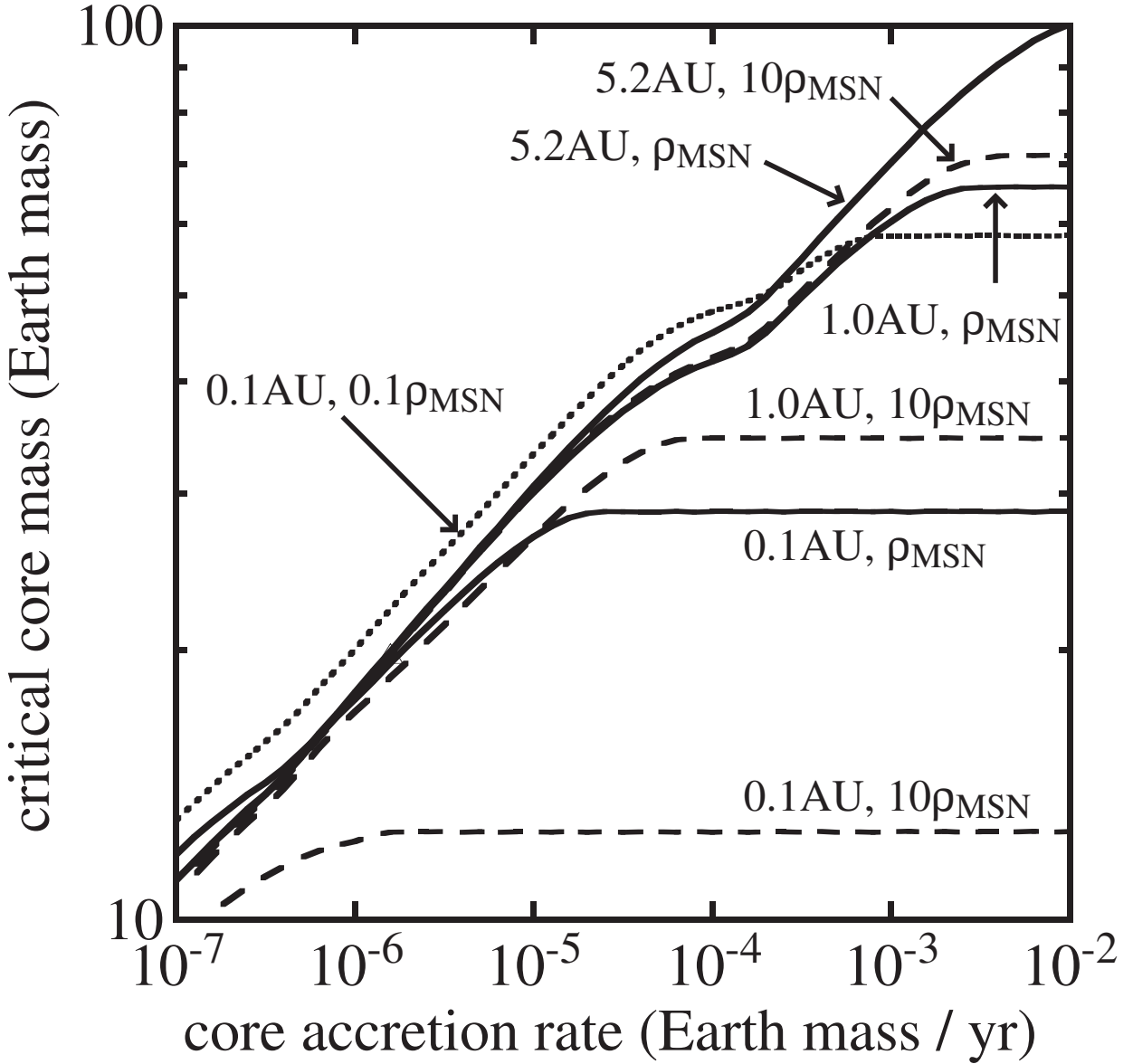


Fig. 3.— The critical core mass as a function of core accretion rate for different choices of distance from the parent star and local density of disk gas.

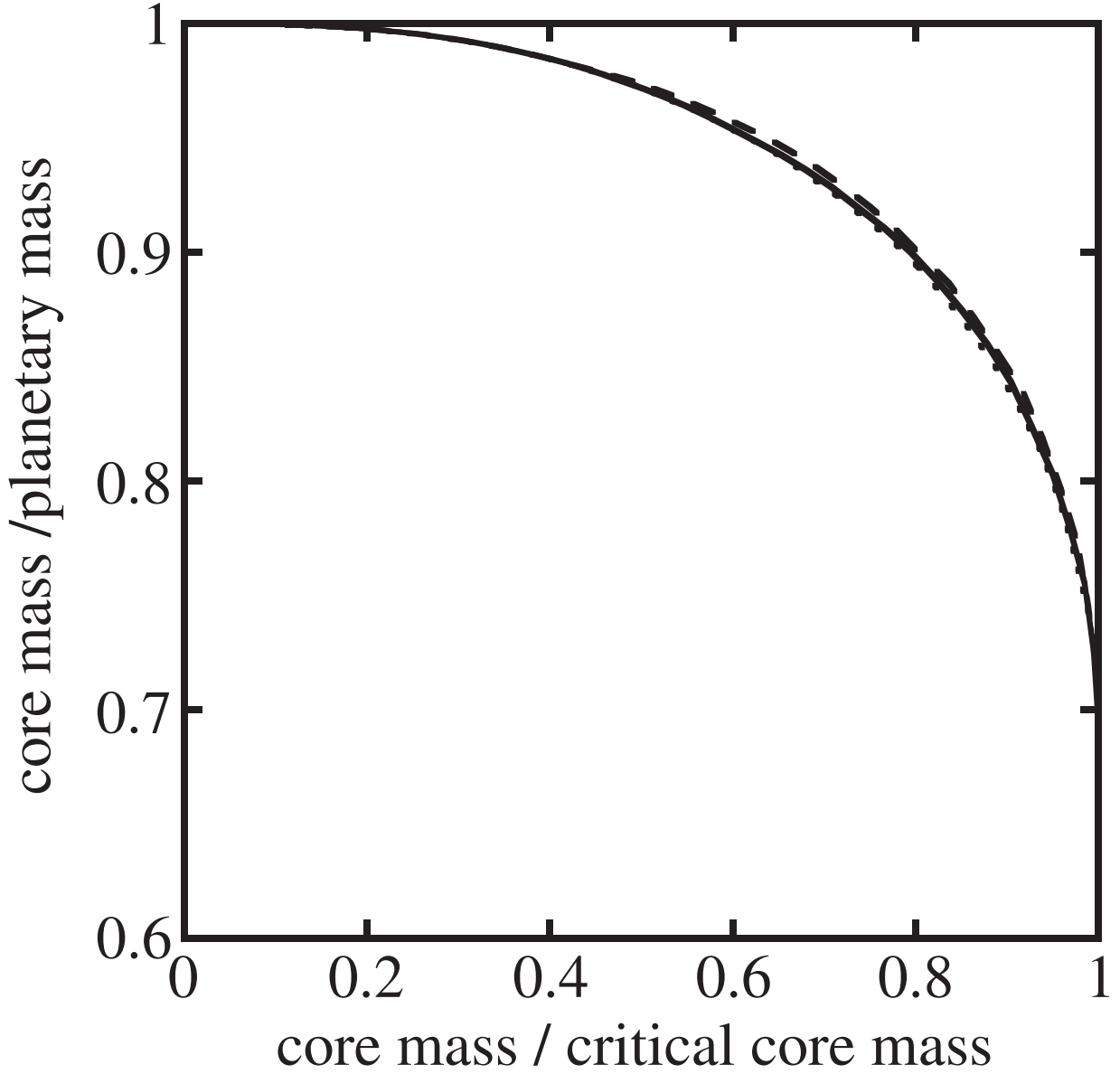


Fig. 4.— The ratio of core mass to planetary total mass as a function of core mass normalized by the critical core mass. The dotted line represents the result for \dot{M}_c of $1 \times 10^{-5} M_{\oplus}/\text{yr}$ at 0.1 AU, the dashed one for \dot{M}_c of $1 \times 10^{-5} M_{\oplus}/\text{yr}$ at 1 AU, and the solid one for \dot{M}_c of $1 \times 10^{-3} M_{\oplus}/\text{yr}$ at 5.2 AU.

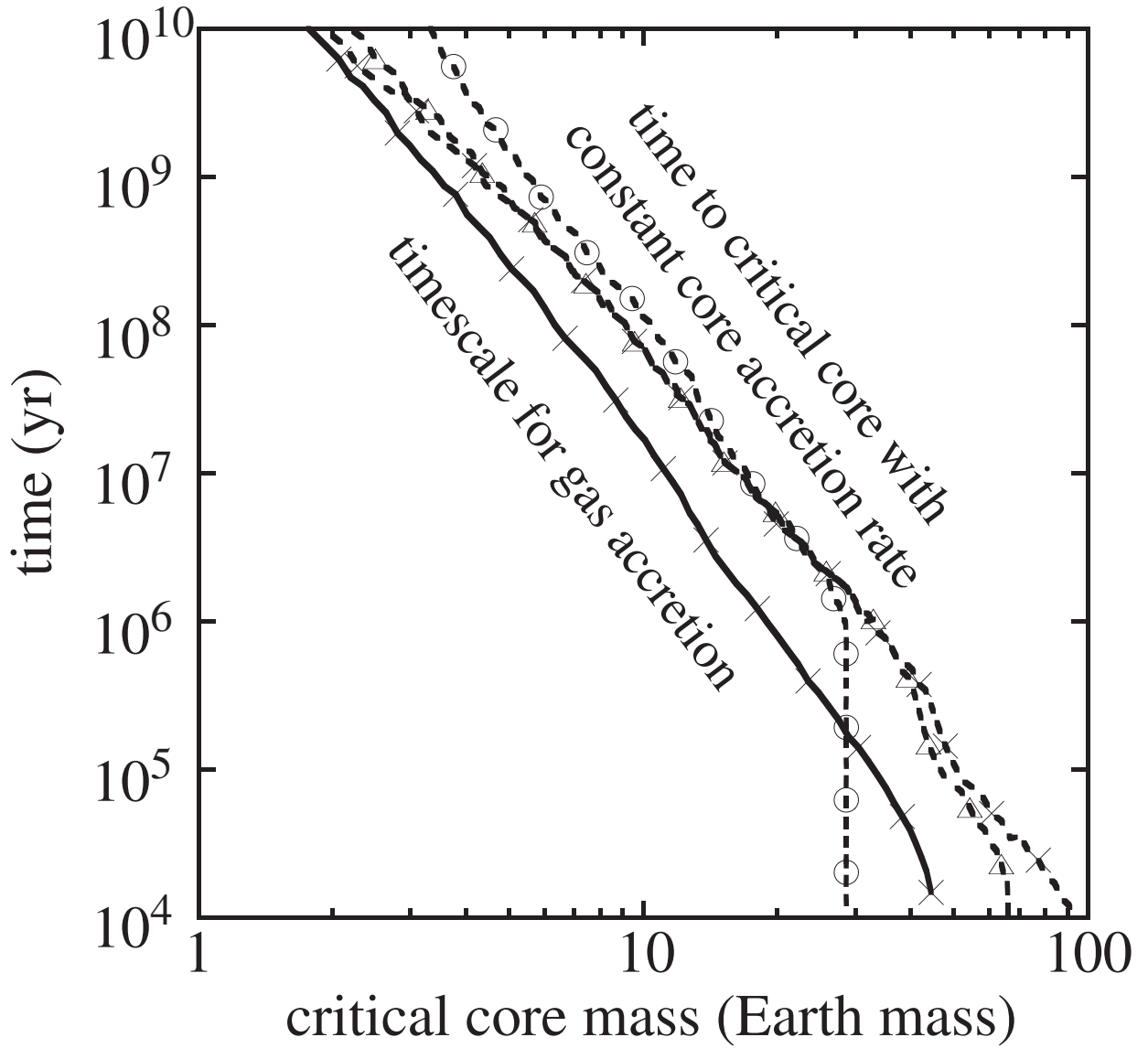


Fig. 5.— Timescale for gas accretion (solid line) is shown as a function of the critical core mass together with time to the critical core (dashed lines). The timescale for gas accretion is that for an e -fold increase in envelope mass just after the critical core mass is attained (see text for the exact definition). The circles, triangles, and crosses are for 0.1, 1, and 5.2 AU in the minimum-mass solar nebula. The vertical part of the dotted curve with circles corresponds to the horizontal part of the corresponding line in Fig. 3.

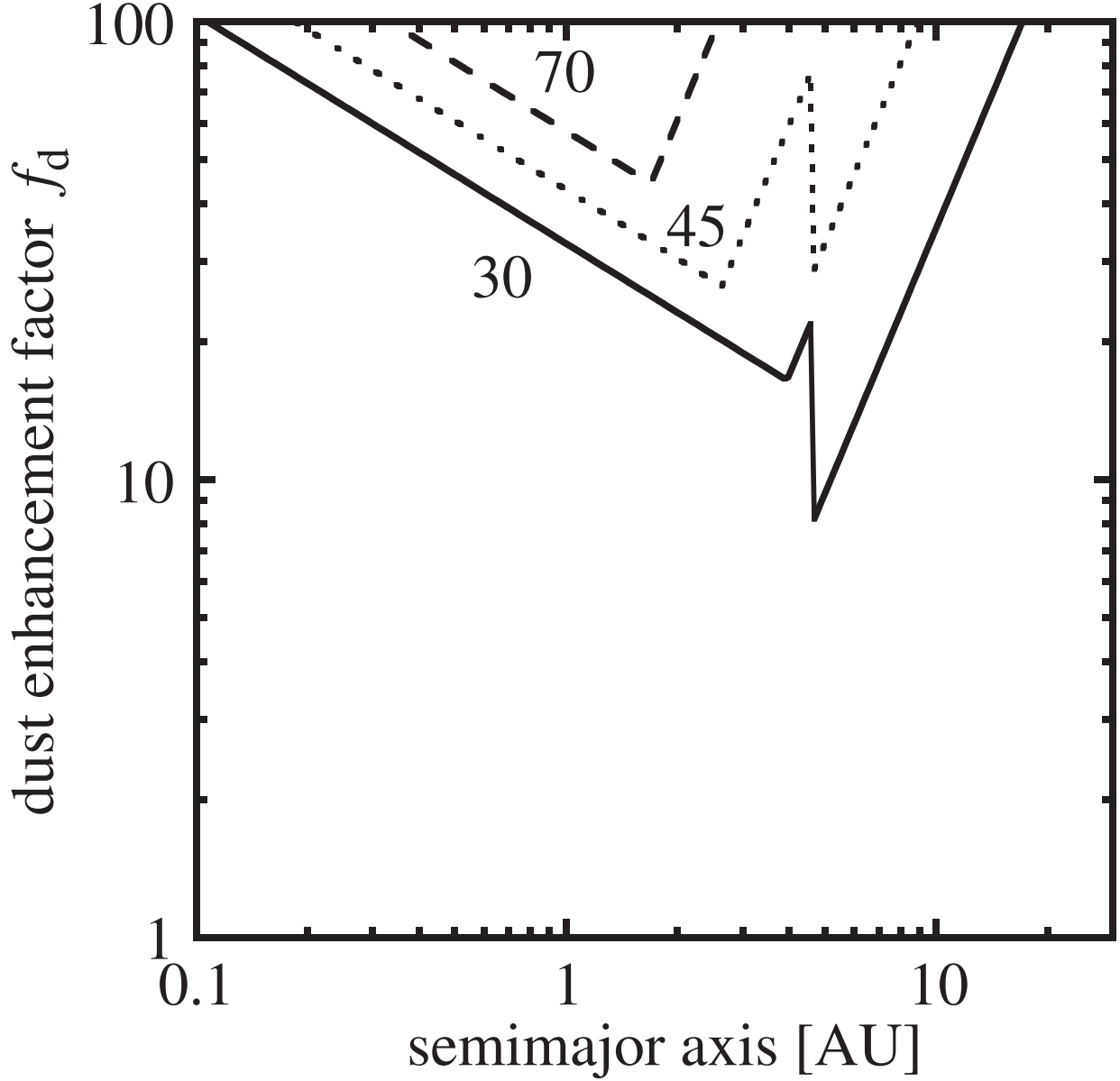


Fig. 6.— The conditions for subcritical core accretion. The subcritical core accretion is possible in the regions over the solid, dotted, and dashed lines for 30, 45 and 70 M_{\oplus} cores, respectively. Corresponding to HD149026, $M_* = 1.3M_{\odot}$ and $[\text{Fe}/\text{H}]=0.36$ ($f_d/f_g = 2.3$) are assumed. Note that the discontinuities of the curves come from sudden increases in disk surface density of dust component at the snow line.

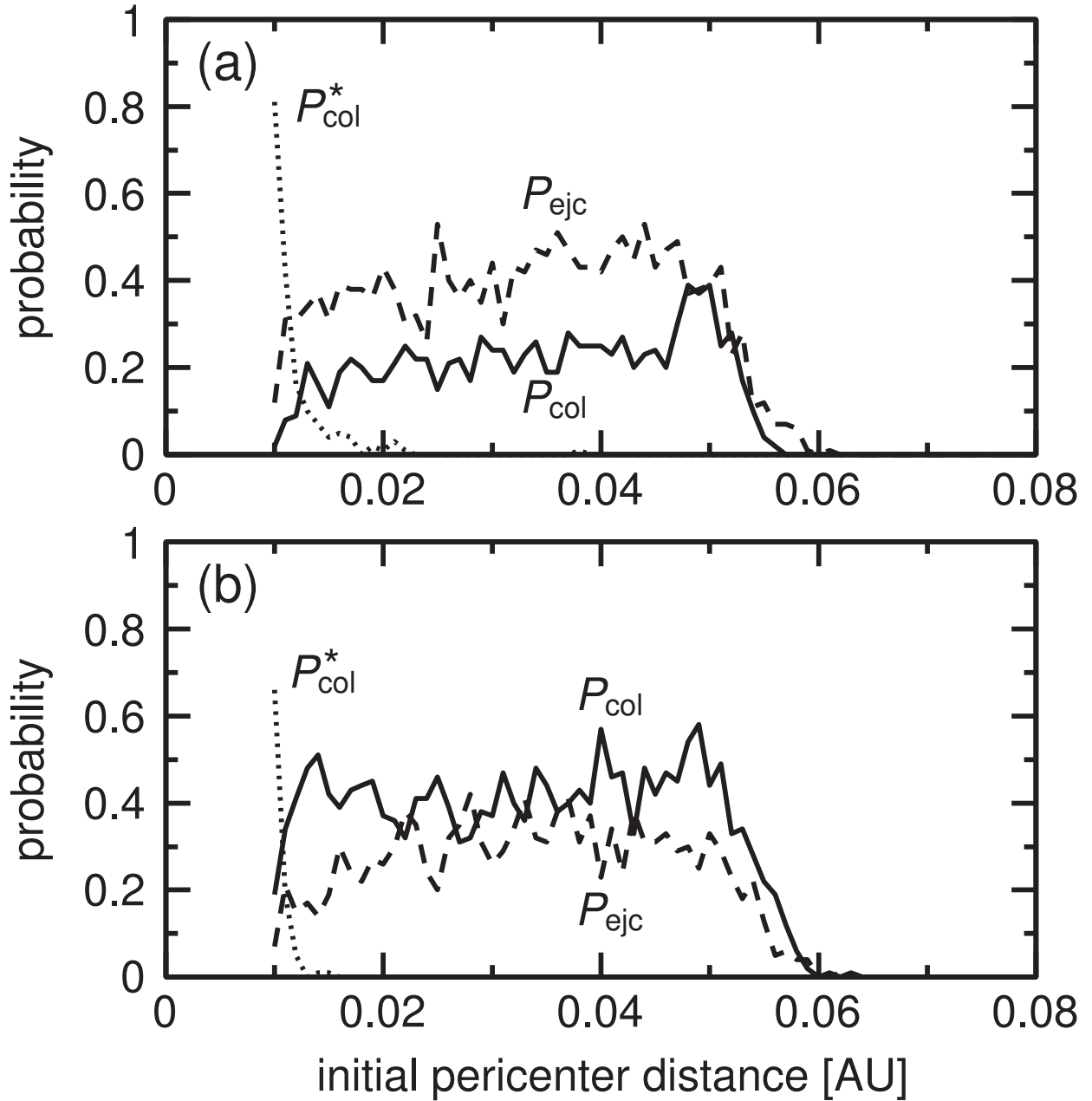


Fig. 7.— Probability of outcomes of encounters between the inner giant planet of $0.5M_J$ in a circular orbit at 0.05 AU and a planetesimal (test particle) (panel a) or another giant planet of $0.5M_J$ (panel b) in a nearly parabolic orbit with initial semimajor axis $a = 1$ AU. For each initial q , 100 cases with random angular distributions are calculated until 100 Keplerian periods at 1 AU. Collision probability with the inner planet (P_{col}), that with the parent star (P_{col}^*), and ejection probability (P_{ejc}) are expressed by solid, dotted, and broken lines. Here, the physical size of planets are determined with internal density 1 g cm^{-3} ; that of the parent star is set as 0.01 AU.

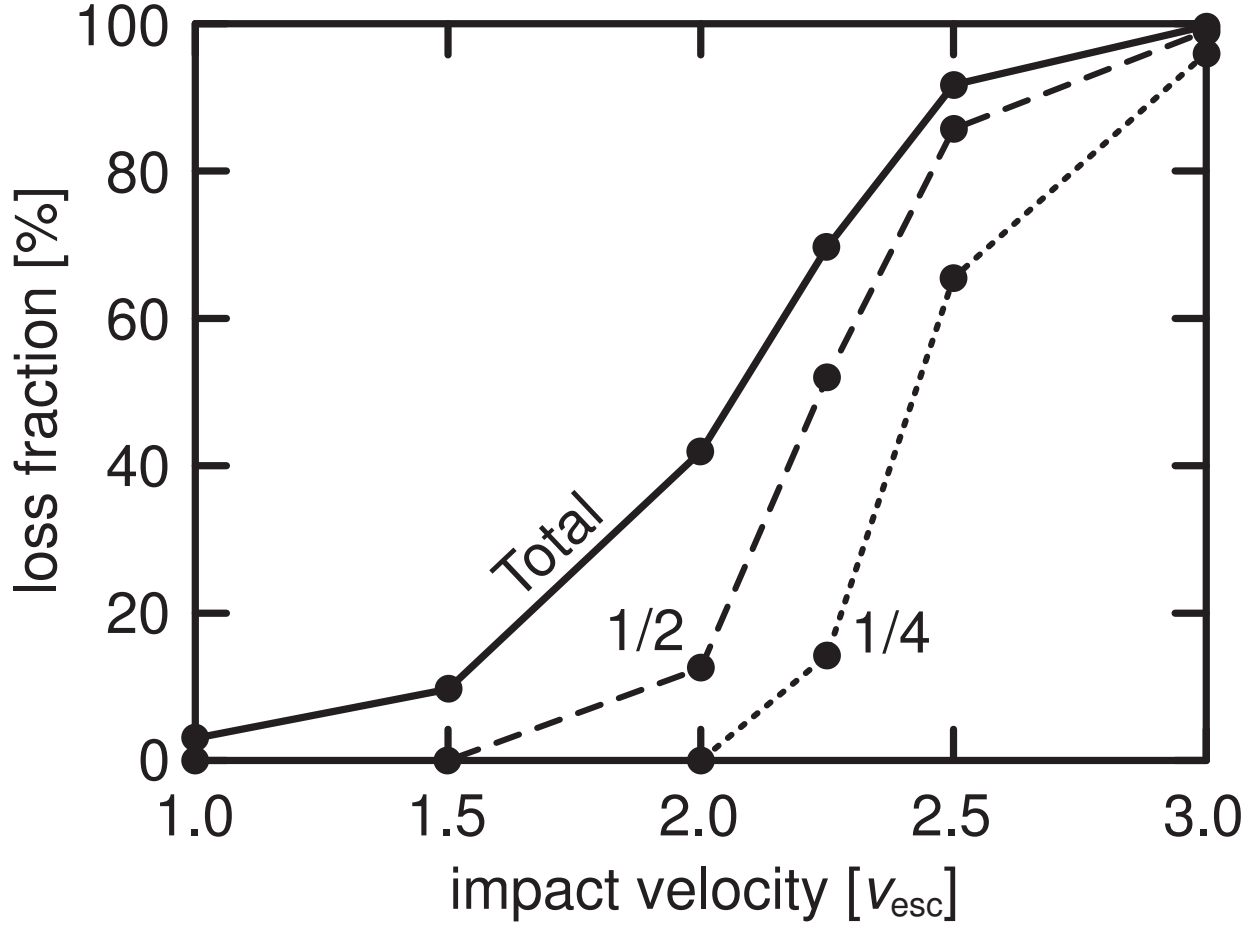


Fig. 8.— The loss fraction of mass after a head-on collision between two Jupiter-mass planets composed of ideal gas with the adiabatic exponent of 2. The loss fraction of mass initially located inside 1/2 (dashed line) and 1/4 (dotted line) of the initial planetary radius are plotted to compare with total loss fraction (solid line). The loss fraction is defined as the mass fraction of the SPH particles whose velocity exceeds the local escape velocity and distance from the center of mass frame exceeds 5 times of the initial planetary radius.